GRAIN SIZE AND TOUGHNESS OF TI-6AL-4V ELECTRON BEAM AND TIG WELD DEPOSITS

Kivineva, Esa[1] and Hannerz, NilsErik[2]

[1]Wärtsilä Corporation, Helsinki, Finland, esa.kivineva@wartsila.com

[2]Royal Institute of Technology, Department of Production Eng.,
Welding Technology, Stockholm, Sweden, nhannerz@iip.kth.se

ABSTRACT
Electron beam (EB) and Gas tungsten arc (TIG) welds were performed on 12.7 mm thick Ti-6Al-4V plate (ASTM Titanium Grade 5). Charpy-V toughness and hardness, as well as, microstructure of the welds and penetration from the macrostructure were studied. It appears that by EB welding rather smaller β-grains than with TIG welding can be obtained. Next to the fusion line the β-grain size in the HAZ was 50 μm while in the weld metal it was 150 μm. Charpy-V toughness of the EB weld metal was equal or even better to that of base metal, which shows that the α-martensite per se is not particularly brittle if only the grain size is fine enough. This is similar to behavior of low carbon martensite in steel. The grain size was studied with light optical and scanning electron (SEM) microscopes. Thus for products, for products which can be manufactured automatically with very narrow fit, the EB welding of Ti-6Al-4V appears to yield satisfactory toughness without any complex post weld heat treatment. In this study as in earlier studies the TIG welds gave lower toughness than that of the base material due to the higher heat input and slower cooling as compared to EB welding.

KEYWORDS
Titanium Grade 5, Ti-6Al-4V, EB welding, TIG welding, Toughness, Microstructure

1 Introduction

The combination of low weight and high strength even at high temperatures, where creep can occur, has made the α-β titanium alloy Ti-6Al-4V an attractive material for aerospace industry. Large amounts of knowledge have been gathered about the material over the years. This Ti alloy, also known as Ti ASTM Grade 5, has been called the workhorse of the titanium industry, as half of the Western world production is in the form of Ti-6Al-4V. As a comparison, the strength of titanium Grade 5 at room temperature is almost five times as that of basic titanium Grade 1 at the same density. TI-6Al-4V is an alternative material for riser tubing in the future North Sea oil wells to be exploited in waters deeper than 100 meters, where with the new techniques, high strength tubes with low weight will be required. The riser tubing can be extruded, but also there would be a possibility to use longitudinally welded tubes. This method for riser tube manufacturing would allow manufacture long tubes and thus reduce transverse filed welds, which have poorer toughness properties.

Titanium is also resistant to most types of corrosion attacks, for instance pitting corrosion in salt water at temperatures encountered in offshore. Titanium is also resistant to corrosion attack types appearing in paper and pulp process environment and actually it appears to be superior even to highly alloyed super duplex and super austenitic stainless steels. Susceptibility to hydrogen embrittlement and hydrogen precipitation is a liming factor for usage of titanium, as is the price of the material. The price has been coming lower and titanium Grade 5 has been becoming an attractive alternative for non-aerospace applications. For offshore and oil well riser tube applications, toughness of longitudinal welds in the welded tubes may become a critical factor. In order to study the influence of the metallographic structure on the toughness it was found that an EB weld would yield to a microstructure with fully α'-phase, which could result in good toughness whereby the limiting influence of the welds could at least be somewhat reduced. For comparison also TIG welds of the same material were studied.

2 Test materials and methods

Test material was 12.7 mm thick titanium Grade 5 plate. The chemical composition of titanium Grade 5 is given in table 1. The material has two alloying elements, i.e., aluminum and vanadium and all other elements should be considered as residuals or contaminants. The ASTM standard gives maximum allowed content for some of the impurity elements, as given in table 1. Aluminum stabilizes the α-phase whereas vanadium acts as β-phase stabilizer.

Titanium, with its large affinity for residuals, picks up carbon, nitrogen, hydrogen and oxygen during processing whereby it may harden. Titanium hydride may also render the material brittle. Yield strength for Grade 5 in annealed condition is approximately 830 MPa, which is almost five times as high as that of unalloyed titanium Grade 1. The yield strength depends on the heat treatment condition being highest approximately 1080 MPa in annealed and aged condition. The ultimate tensile strength in the two cases is 900 and 1140 MPa, respectively. The elongation of titanium Grade 5 in tensile test is decreased from 17.5% to 3.5% as the yield strength increases from 830 to 1080 MPa. Best elongation is achieved with annealing at 845°C followed by aging at 540°C. This will result in 670 MPa in yield strength with 23% elongation. Plate is finish rolled at 955°C to contain lamellar α+β phase structure. To obtain the high strength the material is heat treated above 700°C and thereafter air cooled.

Titanium Grade 5 is typically used with α+β phase structure. The cubic β phase is stable at higher temperatures while at lower temperatures the α+β structure appears. The β transus is about 980°C. Fast cooling from high temperatures will yield to a martensitic hexagonal α' –phase. At heat treatment of the α' structure in the range of 300 to 600°C there will appear hardening when α' precipitates to β. A secondary hardening was also obtained at 593°C and 482°C by Fopiano et.al. [1] which they attributed to α_2 phase (Ti_3Al) precipitation. Slower cooling from the β–range will result in a precipitation of α in the former β grain boundaries. This is followed by a Widmanstätten type precipitation within the grains as the material cools. The Widmanstätten platelets become finer, the more rapid the cooling is. Also, the grain boundary phase in thinner, to disappear completely when quenching. There are no CCT diagrams published with very high solution temperatures. However, an ambitious study with cooling from 1030°C was carried out by LeMaitre [2]. In this work he did not actually quite succeed in obtaining the 100 percent martensitic α' structure, which would need more rapid cooling and a higher peak temperature, as with larger β grains and the α+β -nose would shift to the right.

EB Welding

The EB welding was carried out using Leybold 700/15-60 CNC equipment, which has a maximum 15 kW power at 60 kV acceleration voltage. The vacuum chamber dimensions are 750 x 900 x 1100 mm. High vacuum of 10^{-3}mbar can be obtained in five minutes. The beam can be oscillated in ten different patterns with a function generator. In the present case the beam was oscillated as an ellipse with main axes longitudinal and perpendicular to the welding direction. Amplitude was 0.04 mm in the X-direction (welding direction) and 0.22 mm in the Y-direction perpendicular to the welding direction. Oscillation frequency was 1000 Hz.

According to Matsuda and Hashimoto [3] the penetration would be similar for titanium and iron at high welding speed, where higher proportion of the thermal energy is used for melting. At the rate of 5 mm/s, however, the penetration would be about 10 percent higher and at 10 mm/s welding speed the penetration would be 8 percent higher for titanium as compared to steel. The authors have made theoretical calculations followed by experiments to confirm the findings. Based on this, larger penetration with EB welds with normal welding speeds would be expected in titanium compared to steel. In the experiments it was observed that approximately 75 percent of the heat input was needed with titanium in EB welding to get the same penetration as with SS2172 steel. It has been given in the literature from the 70s that penetration at 120 – 150V and 5.5 – 6.5 mA would be 6.3 mm for titanium Grade 5 and 4.3 mm for 4340 steel. Hablanian [4] has considered different factors such as thermal conductivity and melting point and obtained a straight line for the relation:

$$b = \frac{CP}{T_k}\sqrt{\frac{k}{Vd}} \qquad (1)$$

where b is penetration, P is power T_k is melting point, k is thermal diffusivity and v is welding speed.

Passoja [5] suggested that penetration would be proportional to the heat of vapor formation. However, he never gave any experimental evidence. In recent approach to the problem Hemmer and Grong [6] used the evaporation temperature when treating the penetration depth as the depth of the keyhole thereby considering the influence of the evaporation.

The test welds were done bead on plate with two passes to have equal conditions as in the real situation. The first pass was a rapid only partial penetrated weld to simulate tack weld normally holding the pieces together. The second

pass was welded within 10 second after the first one aiming a fully penetrated joint. The test weld situation has been illustrated in figure 1. Figure 2 shows macrographs of test welds on the plate. Welding parameters used are given in table 2. Parameters of test weld number 6 were used with a real butt joint preparation using square edge preparation and parameters as given in table 2. This set up gave full 12.7 mm penetration with very few protrusions in the root. From the test weld number 6 Charpy-V specimens were manufactured with notch located in the centre of fused metal.

TIG welding
Welding was performed with the ESAB Protig 450 equipment, which allows separate programming of voltage, ampere and welding speed. The TIG welding was carried out with two passes bead on plate with shielding gas in the root and a chamber filled with shielding gas trailing the arc. The bead on plate passes were welded one on each side using same parameters. The parameters are given in table 2. Each weld was almost fully penetrating, beads overlapping in the middle of the plate. Charpy-V specimens were manufactured from the TIG welded plate with notch located in the fused metal.

The base material Charpy-V toughness was tested both perpendicular and transverse to the rolling direction. The results were almost equal and no directionality could be observed in the toughness of the base plate. The Charpy-V test results for base material and EB and TIG welds can be seen in figure 3.

Welds were polished and etched in HF + HNO_3 solution at room temperature. Hardness of the EB welds was measured with a Vickers method and the grain size was measured by linear intercept method. The grain sizes can be seen in table 3 and an example of a hardness profile in figure 4. Microstructures of base material, heat affected zone (HAZ) and weld metal can be seen in figure 5. Fracture surfaces were studied with SEM. The fracture images for base material can be seen in figure 6 and for EB weld in figure 7.

3 Results and discussion
EB weld metal consists of large conserved β grains α' phase, i.e., hexagonal martensite phase. HAZ is rather wide as a result of relatively low β transus. It was observed that the grain size in the HAZ was rather small, smaller than expected, which may be associated to steep temperature gradient during welding. Similar effect has been pointed out in earlier work [7] when the grain growth in titanium was studied at Gleeble simulation. In that study, the lowest β grain size of 192 μm was obtained with cooling rate $\Delta t_{8/5}$ of 10 s. Now the measured EB weld metal grain size was only 50 μm, which would mean cooling rate of $\Delta t_{8/5}$ of 2 s. Cooling time in the weld metal was not measured but when applying Arata's formula [8], $\Delta t_{8/5}$ values of 0.4 – 0.5 can be calculated giving an order of magnitude for the cooling rate. At this rapid cooling the resulting microstructure will be α' martensite. As a comparison, in the earlier work [7] plasma welds were manufactured with cooled copper blocks on both sides of the bead resulting in grain sizes of 375 μm in the weld metal. The cooling time $\Delta t_{8/5}$ would be an order of magnitude longer for the TOG welds as compared to that of the EB welds.

It appears that the toughness of the EB welds is well above of that of the base material in room temperature and higher. The toughness is equal approximately at -70°C temperature. As expected the Charpy toughness of the TIG welds is below that of the base material in the test temperatures.

SEM investigation of Charpy-V specimen fracture surfaces revealed a rock candy looking but in reality consisting of large but flat dimples. This was the case in the lowest temperatures were the toughness was not higher than 12 J. At the highest temperature with Charpy-V values above 50 J, fracture surfaces were ductile tearing type with smaller dimples particularly within the β grains. At approximately same toughness energy values the base material fracture surface would look more cleavage like with river patterns. No sharp transition in ductility was observed with the test material.

4 Conclusions
It is concluded that EB welding of titanium Grade 5 results in welds that have toughness equal or better than the base material. The TIG welds had toughness clearly below those of EB welds and base material. The results would suggest that it would be possible to apply EB welding on longitudinally welded pipes. Other welding methods would require costly post weld heat treatment to achieve adequate toughness levels. Another interesting application of EB would be airplane fuselages, which may come true with the new generation fighter planes [9].

Acknowledgements

The authors wish to thank Mr. P. Kellgren of Permascand for the test material used in this investigation. Mr. R. Heiskanen is thanked for his knowledge support, as well as, for welding the test material. Volvo Transmission is acknowledged for usage of their EB welding equipment, and ESAB AB who set the TIG equipment at our disposal. Mr. Hu Limu made the metallographic investigation of the EB welds. Also the aid with TIG welding was obtained from Mr. C. Larsson and Mr. P. Kihlmark.

References

[1] P.J. Fopiano, M.B. Bever and B.L. Averbach: Phase transformation and strengthening mechanisms in the alloy Ti-6AL-4V. Trans ASM Vol 62 (1969). pp 324-332

[2] F. LeMaitre: Etude des transformations en refoidissement continu de l´alliage de titane Ti-A6V. Memoir Scientifique Rev Metallurgique. Vol 67 (1970) No. 9. pp. 563-574

[3] T. Hashimoto and F. Matsuda: An equation for calculating welding condition in electron beam welding. Trans Nat (Jap) res Inst for Metals Vol9 (1967) No.1. pp 48-53

[4] M.A. Hablanian: A correlation of welding variables. Proc Electron Beam Symp 5th Ann Meeting Boston Mass 1963. pp 262-268

[5] D.E. Passoja: Penetration of solids by high power density electron beams. Brit Weld Journ Vol 14 (1967) No.1. pp 13-16

[6] H. Hemmer and O. Grong: Prediction of penetration depths during electron beam welding. Science and Technology of Welding and Joining Vol 4 (1999) No. 4. pp 219-225

[7] E. Kivineva, NE. Hannerz and R. Sjöberg: Microstructure of Ti 6Al 4V weld metal and simulated HAZ. Proc Offshore Materials and Arctic Engineering OMAE 1995 Copenhagen, Vol III, Materials Engineering. pp 401-407

[8] F. Matsuda, F.T. Hashimoto and Y. Arata: Some metallurgical investigations on electron beam welds. Trans Jap Weld Soc Vol 1 (1970) No 1. pp 1-14

[9] B. Irving: EB welding joins the titanium fuselage of Boeing F-22 Fighter. Welding Journal Vol 73 (1994) No. 12. pp 31-36

Table 1. Analysis of Ti6Al4V in wt-% according to the ASTM standard.

C_{max}	Al	V	Fe_{max}	O_{max}	N_{max}	H_{max}
.10	5.5 – 6.75	3.5 – 4.5	.40	.20	.015	.05

Table 2. Welding parameters used.

Weld	First pass			Second pass			Penetration
	U_{acc} [kV]	I_b [mA]	V [mm/s]	U_{acc} [kV]	I_b [mA]	v [mm/s]	[mm]
1	60	30	40	60	31.0	10	9.7
2	60	30	40	60	33.5	10	11.1
3	60	30	40	60	36.0	10	12.5
4	60	30	40	60	34.5	10	11.5
5	60	30	40	60	32.5	10	10.7
6	60	30	40	60	37.5	10	12.7
TIG	15 V	350 A	1.8	15 V	350 A	1.8	

Table 3. Grain sizes of EB welds and HAZ.

	Grain size in weld	Grain size in HAZ	Width of HAZ
	[μm]	[μm]	[μm]
Base material	16		
Weld 1	154	24	840
Weld 2	189	30	812
Weld 3	176	44	905
Weld 4	160	39	756
Weld 5	160	42	1120
Weld 6	160	30	720

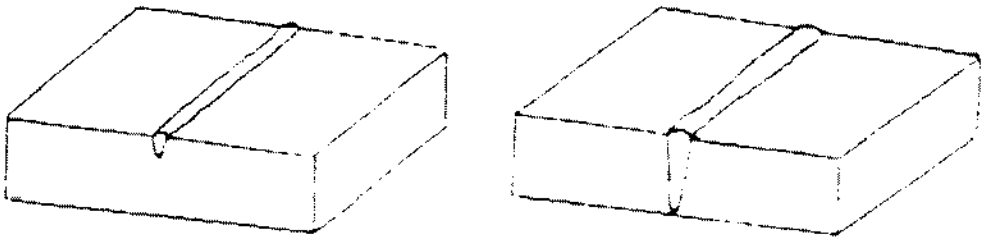

a) b)

Figure 1. Illustration of test weld situation a) first pass simulating tack weld and b) second pass with through thickness penetration.

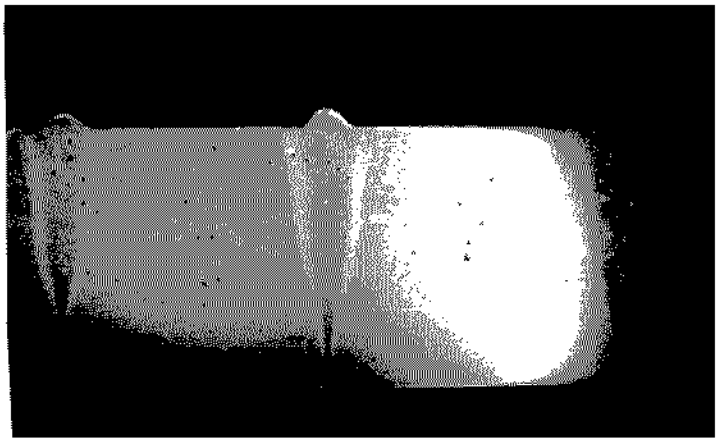

Figure 2.. Macrographs of EB test welds.

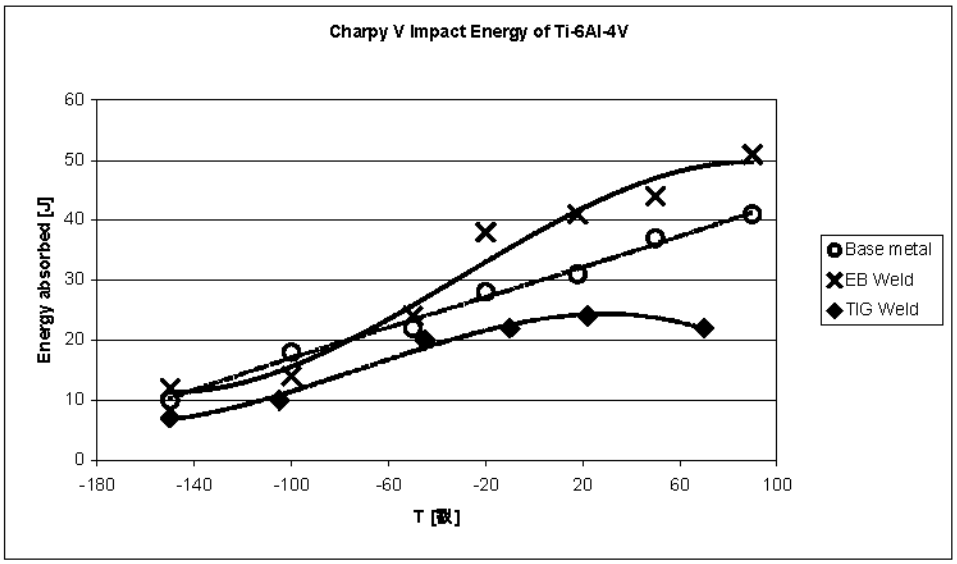

Figure 3. Charpy-V curves for base material, EB welds and TIG welds.

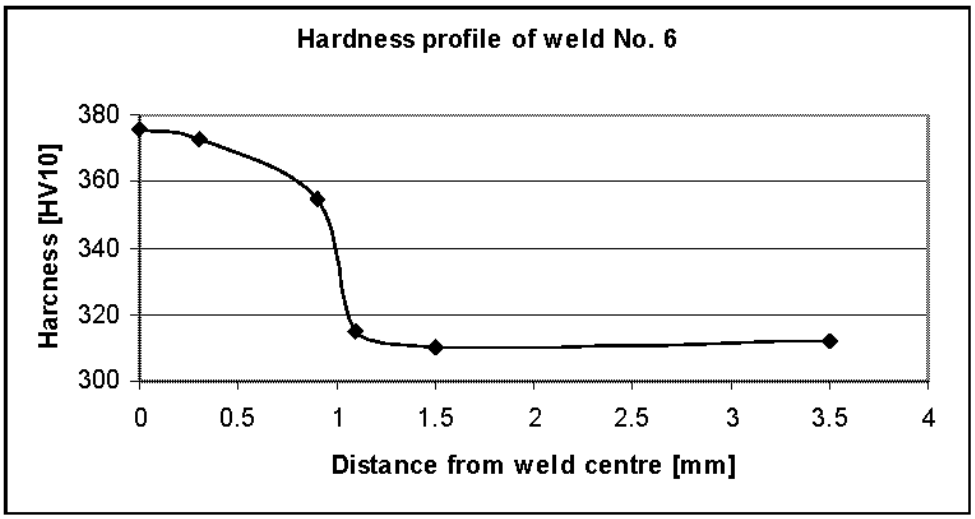

Figure 4. Hardness profile of an EB weld.

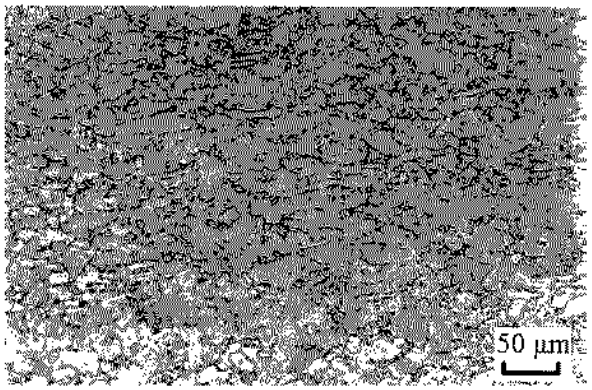

a)

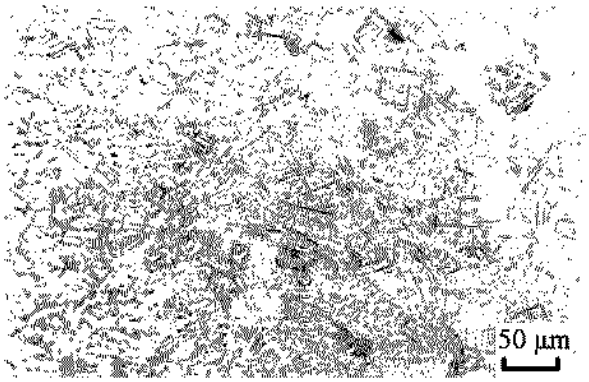

b)

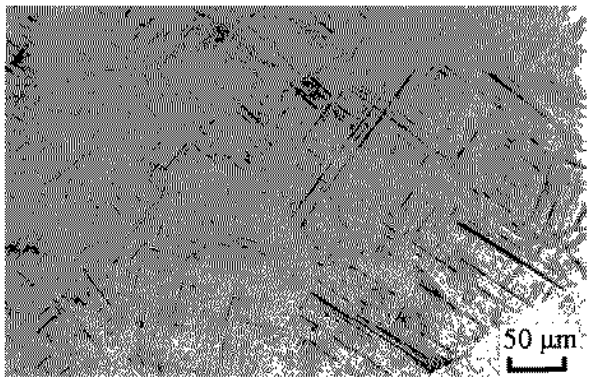

c)

Figure 5. Microstructure of a) base material, b) heat treated zone (HAZ) and c) weld metal.

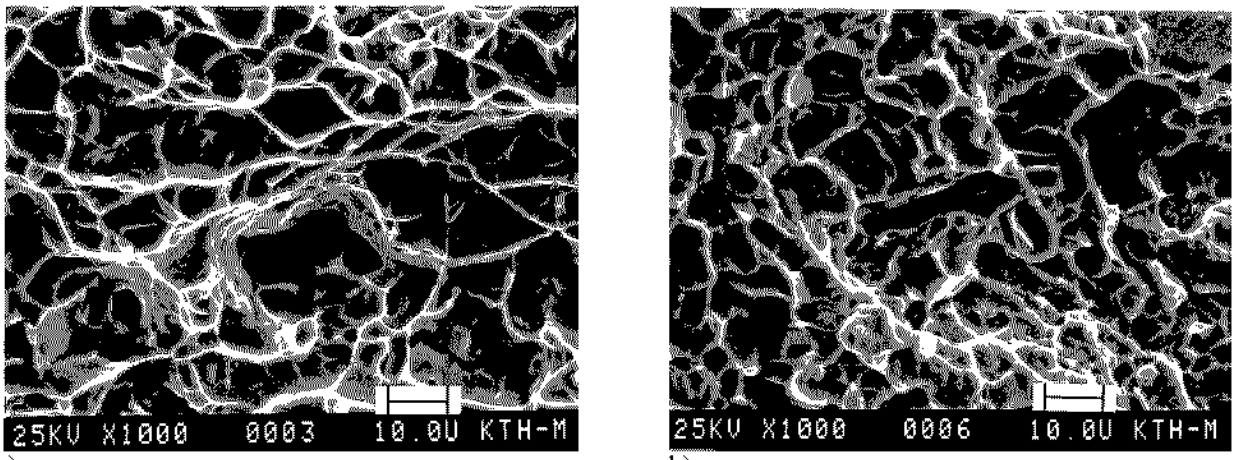

a) b)

Figure 6. SEM images of base material Charpy-V fracture surfaces tested at a) +90°C and b) –150°C

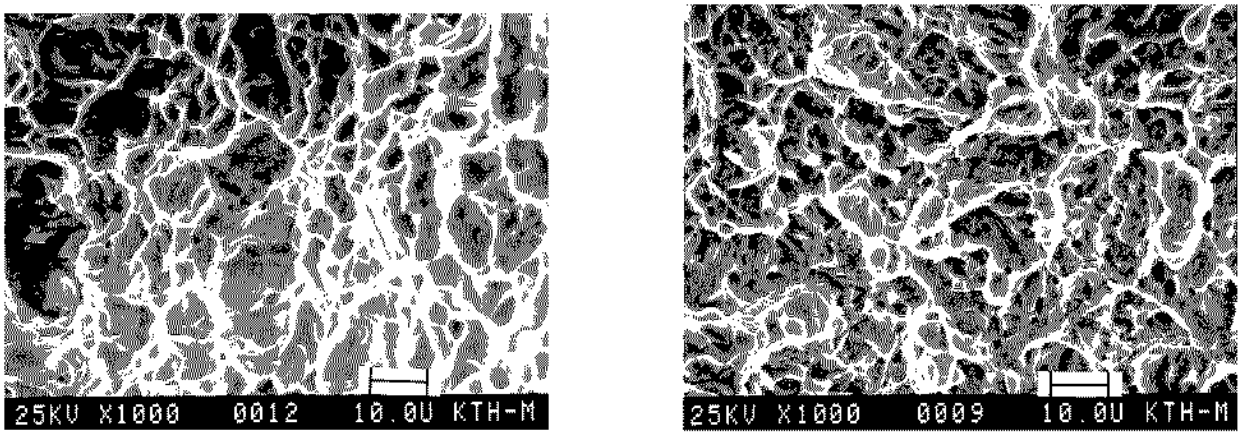

a) b)

Figure 7. SEM images of EB weld Charpy-V fracture surfaces tested at a) +90°C and b) –150°C